Biochimica et Biophysica Acta 1840 (2014) 1738–1746

Contents lists available at ScienceDirect

Biochimica et Biophysica Acta

journal homepage: www.elsevier.com/locate/bbagen

Antarease-like Zn-metalloproteases are ubiquitous in the venom of different scorpion genera

Ernesto Ortiz [a], Martha Rendón-Anaya [b], Solange Cristina Rego [c], Elisabeth Ferroni Schwartz [c], Lourival Domingos Possani [a,*]

[a] Departamento de Medicina Molecular y Bioprocesos, Instituto de Biotecnología, Universidad Nacional Autonóma de México, Avenida Universidad 2001, Cuernavaca 62210, Mexico
[b] Laboratorio Nacional de Genómica para la Biodiversidad, Centro de Investigación y de Estudios Avanzados del Instituto Politécnico Nacional, Km 9.6 Libramiento Norte Carretera León, Irapuato, Guanajuato 36821, Mexico
[c] Departamento de Ciências Fisiológicas, Instituto de Ciências Biológicas, Universidade de Brasília, Brasília, DF 70910-900, Brazil

ARTICLE INFO

Article history:
Received 17 October 2013
Received in revised form 28 November 2013
Accepted 9 December 2013
Available online 19 December 2013

Keywords:
Antarease
cDNA library
Pancreatitis
Scorpion
Zn-metalloprotease

ABSTRACT

Background: The venoms of several scorpion species have long been associated with pancreatitis in animal models and humans. Antarease, a Zn-metalloprotease from *Tityus serrulatus*, is able to penetrate intact pancreatic tissue and disrupts the normal vesicular traffic necessary for secretion, so it could play a relevant role in the onset of acute pancreatitis.
Methods: The cDNA libraries from five different scorpion species were screened for antarease homologs with specific primers. The amplified PCR products were cloned and sequenced. A structural model was constructed to assess the functionality of the putative metalloproteases. A phylogenetic analysis was performed to identify clustering patterns of these venom components.
Results: Antarease-like sequences were amplified from all the screened cDNA libraries. The complete sequence of the antarease from *T. serrulatus* was obtained. The structural model of the putative antarease from *Tityus trivittatus* shows that it may adopt a catalytically active conformation, sharing relevant structural elements with previously reported metalloproteases of the ADAM family. The phylogenetic analysis reveals that the reported sequences cluster in groups that correlate with the geographical localization of the respective species.
Conclusions: Antareases are ubiquitous to a broad range of scorpion species, where they could be catalytically active enzymes. These molecules can be used to describe the evolution of scorpion venoms under different ecogeographic constrains.
General significance: For the first time the complete sequence of the antareases is reported. It is demonstrated that antareases are common in the venom of different scorpion species. They are now proposed as targets for antivenom therapies.

1. Introduction

It is well known that certain scorpion stings are associated with acute pancreatitis in humans. In particular, the stings from the *Tityus* species produce abdominal pain, nausea and vomiting and in many cases development of acute pancreatitis. After the first clinical cases were reported by Waterman in 1938 [1] for accidents involving the Trinidadian scorpion *Tityus trinitatis*, other reports confirmed the linkage between scorpion poisoning and acute pancreatitis for this species [2,3]. The venoms from other species of the *Tityus* genus, as well as some of their fractions and isolated components have been shown to produce pancreatitis or morphological changes associated with it. That is the case for *Tityus asthenes* from Colombia, which induced acute pancreatitis in children [4], *Tityus serrulatus* from Brazil as tested in dogs, rats and guinea pigs [5–8] and *Tityus discrepans* from Venezuela in mice [9]. Light microscopy of pancreas from *Tityus zulianus*-envenomed mice revealed interstitial edema and vacuolization of acinar cells [10]. Acute pancreatitis has also been documented in children stung by *Leiurus quinquestriatus* from Israel [11,12]. It has been shown that the *Mesobuthus tamulus* venom acts directly on exocrine pancreas to cause acute pancreatitis to anesthetized dogs and rabbits [13].

Paul Fletcher's group, working at East Carolina University, showed that venoms from *Tityus* scorpions are potent secretagogues that can elicit the release of secretory proteins from the exocrine pancreas [5,8,14,15] and neurotransmitters from synaptosomes [15]. Purified toxins or whole venoms from *T. serrulatus*, *Tityus bahiensis* and *Tityus stigmurus* trigger exocytosis in a dose-dependent manner [5,8,15]. Morphological studies by microscopy of pancreatic acinar cells after

Abbreviations: ADAM, a disintegrin and metalloproteinase; BLAST, basic local alignment search tool; HMM, hidden Markov model; MD, molecular dynamics; NPT, constant-temperature, constant-pressure ensemble; PDB, protein data bank; PSI-BLAST, position-specific iterative BLAST; Rgyr, radius of gyration; SVMP, snake venom protease, SNARE, soluble N-ethylmaleimide-sensitive factor attachment protein receptors; TsTX, tityustoxin

* Corresponding author. Tel.: +52 777 3291647.
E-mail address: possani@ibt.unam.mx (L.D. Possani).

0304-4165/$ – see front matter © 2013 Elsevier B.V. All rights reserved.
http://dx.doi.org/10.1016/j.bbagen.2013.12.012

treatment with purified toxins or the whole venom from *T. serrulatus* reveal not only a dramatic decrease in the number of zymogen granules due to the induced discharge, but also other cellular changes such as vacuolization, interstitial swelling, partial effacement of the acinar lumen, loss of microvilli, and the appearance of secretory material and cellular debris in the lumen, suggesting the loss of structural integrity. These events have been associated to acinar cell damage and proposed to be possible early events ultimately progressing to the cellular necrosis of acute pancreatitis observed in vivo after *T. serrulatus* intoxication [8,14]. The effects of "tityustoxin" ("TsTX"; [16]), a heterogeneous fraction from *T. serrulatus* venom [17], on the pancreatic secretion of rats were investigated by Novaes et al. [7]. TsTX did not change the serum levels of lactate dehydrogenase, thus suggesting that this particular alteration induced by the whole venom is due to other component(s) of the venom, acting alone or synergistically with TsTX. Though isolated toxins are capable of eliciting the secretory response of the acinar cells, it has been speculated that the clinical manifestations of acute pancreatitis observed with the whole venom could be the result of the synergistic action of several components of the venom [7,8] as the neurotoxins that act indirectly on the pancreatic function by stimulating the liberation of acetylcholine in the pancreatic nerve terminals [18,19].

The most significant venom components in terms of their abundance, physiological effects and medical consequences, are ion channel-modulating toxins. But scorpion venoms are a rich source of other biologically active molecules. These include some enzymes. To date, several enzymatic activities have been characterized in scorpion venoms, including phospholipase A [20,21], hyaluronidase [22], sphingomyelinase D [23], lysozyme [24] and gelatinolytic/caseinolytic proteases, mostly serine-proteases [25]. Two mRNA sequences coding for putative Zn-metalloproteases from the Asian scorpion *Mesobuthus eupeus* have been submitted to GenBank (Accession numbers EF442045.1 and EF442046.1). The presence of proteases in the scorpion venoms has been associated with the facilitation of venom permeation into tissues [25] and the posttranslational processing of toxin precursors [26].

It was very recently that a novel zinc-metalloprotease, named antarease, was purified from the venom of *T. serrulatus* and characterized [27]. It constitutes the first example of a scorpion protease with a potentially pathogenic mechanism of action. Antarease appears to penetrate intact tissue and specifically cleave the soluble N-ethylmaleimide-sensitive factor attachment protein receptors (SNAREs) involved in pancreatic secretion, thus disrupting the normal vesicular traffic. Due to its activity, antarease might be one of the components responsible for the onset of acute pancreatitis observed after *T. serrulatus* intoxication. If this proves to be the case, this protease should be considered as a therapeutic target for the generation of antivenoms able to neutralize the toxic effect of the whole venom, an effort that has until now focused on the ion-channel modifying toxins [28,29]. It was recently shown that the venoms of the Brazilian scorpions *T. serrulatus*, *T. stigmurus* and *T. bahiensis* are able to cleave dynorphin 1–13, an activity associated with metalloproteinases. The finding that the two Brazilian antivenoms used for human therapy poorly neutralize the dynorphin 1–13 cleavage activity of those venoms reinforces the idea that better antivenoms are still needed [30].

The reported sequence of the antarease was determined by direct Edman sequencing of the N-terminus and of peptides derived from several proteolytic cleavages. Despite the fact that this finding was quite original, describing important structural features and possible functions of an enzyme that might play a crucial role on human pancreatitis caused by scorpion stings [27], the sequence reported is nevertheless incomplete, with about 10% of its amino acid sequence not determined. In addition, small sequence differences were found when analyzing the sequence reported in the original paper and the one in the UniProt Database (accession number P86392). Given the importance that this enzyme might have on acute pancreatitis, we consider relevant to determine its complete precise amino acid sequence. The total amount of this enzyme present in *T. serrulatus* soluble venom, based on chromatographic separation and mass spectrometry analysis, indicates that this enzyme is around 0.5% of the whole soluble venom. For sequencing analysis we used a molecular biology approach, looking for the sequence of this protein-coding mRNA.

Since acute pancreatitis has also been observed for other scorpion venoms, we set to look for similar sequences in cDNA libraries of other species of the *Tityus* and *Centruroides* genera to which we have access. Additional to the findings described here concerning the primary structure of antarease and antarease-like enzymes from different species of the genus *Tityus* it is worth mentioning that analysis of the evolutive role of these enzymes in scorpion venoms is also an original part of this communication.

2. Experimental

2.1. cDNA library construction

The cDNA library from the venom glands of *Tityus trivittatus*, constructed with the SMART cDNA Library Construction Kit (Clontech) was described before [31].

For this work new cDNA libraries were constructed from the telsons of individual specimens of *T. serrulatus*, *Tityus fasciolatus*, *Tityus pachyurus* and *Tityus* sp. This last is yet an undescribed *Tityus* species from Colombia, collected in Popayán (Cauca), Colombia (2°26′39″N, 76°36′18″W). For total RNA extraction the ZR RNA MiniPrep Kit (Zymo Research) was used following the instructions from the manufacturer. The total RNA was quantified by absorbance with a NanoVue Spectrophotometer (GE Healthcare, Life Sciences). Further, the In-Fusion SMARTer cDNA Library Construction Kit (Clontech) was used to construct the cDNA library. For first strand amplification, 0.5 μg of total RNA was employed. The double-stranded cDNA was amplified (RT-PCR) from 2 μl of the previous reaction, fractioned by size through a CHROMA-1000 column and quantified by absorbance. Nine hundred nanograms of ds-cDNA were ligated to 300 ng linearized pSMART2IF vector and electrotransformed into electrocompetent DH5α cells.

2.2. Primer design, PCR amplification and cloning

The available protein sequence of the antarease from *T. serrulatus* (SwissProt P86392.1) was backtranslated with full degeneracy. Within the generated sequence a search was performed to identify specific regions with the lowest possible degeneracy that could function as primers. Two regions were identified close to the 5′ and 3′ ends of the degenerated sequence and for them primers were designed: AntUp1, 5′-GAYGAYTGYATHGTNGTNGARTAYTAYAT-3′ (29-mer, tm = 52.6–65.7 °C, degeneracy = 3072, all calculations made with Oligo v7.54) and AntLw2: 5′-RTCNSWRCAYTGYTGRAADATRCA-3′ (24-mer, tm = 51.7–63.3 °C, degeneracy = 3072). Y = G/C, H = A/T/C, N = A/T/G/C, R = A/G, S = G/C, W = A/T, D = A/G/T.

The *Tityus trivittatus* cDNA library was constructed with the pDNR-LIB vector (Clontech), so a combination of the above degenerated primers and T7DIR (5′-GTAATACGACTCACTATAGGG-3′) or M13REV (5′-AACAGCTATGACCATGTTCAC-3′) specific for the vector, were used for amplification. The PCR conditions were 5 min 94 °C, followed by 30 cycles of 30 s 94 °C, 1 min 50 °C, 1 min 72 °C, plus an extension step of 5 min, 72 °C. *Pfu* Polimerase was used (Fermentas). The product was purified by PAGE/QIAquick Gel Extraction Kit (QIAGEN), blunt cloned into pBluescriptKS(+) and electrotransformed into competent DH5alpha cells. Positive clones were selected and sequenced. A partial sequence was obtained for the cDNA that was lacking the 5′ region of the mRNA. From this sequence, the primer AntTtrLw3 (5′-ATTCCCAG CTCCAACGTATCCATC-3′) was designed and used in combination with the T7DIR primer to amplify the remaining sequence from the *T. trivittatus* library. The PCR conditions and cloning procedure were the same as above.

The *T. serrulatus*, *T. fasciolatus*, *T. pachyurus* and *Tityus* sp. cDNA libraries were constructed with the pSMART2IF vector (Clontech), so the Forward (5′-TCACACAGGAAACAGCTATGA-3′) and Reverse (5′-CCTCTTCGCTATTACGCCAGC-3′) Screening Primers provided by the cloning kit were used in combination with our degenerated primers to amplify the sequences from the libraries. The PCR conditions were 5 min 94 °C, followed by 35 cycles of 30 s 94 °C, 1 min 42 °C, 1 min 72 °C, plus an extension step of 5 min, 72 °C. *Pfu* Polimerase was used (Fermentas). The purification and cloning steps were the same as above.

2.3. Molecular modeling

The attempt to build the model of TtrivMP_A by comparative modeling was hampered by the low coverage and identity (45% and 31%, respectively) of the highest-ranked homologous protein with crystallographic structure (PDB ID 2W12) identified by BLAST [32]. With such low sequence coverage, we decided to adopt the fold recognition approach for identifying potential templates by the Phyre2 server [33] for molecular modeling. This server is able to identify homologues using distant profiles sequences obtained from algorithms such as PSI-BLAST [34] and HMM [35]. Thus, several models were suggested with 100% confidence values, of which the one with the highest score was chosen (the one based on template PDB ID 3K7N, 2.3 Å resolution). As the server Phyre2 also uses ab initio methods to construct regions for which it does not recognize a folding pattern, the model was subjected to refinement by molecular dynamics simulations. Before submitting the model to the simulation, a zinc ion was added to the predicted metal-binding site.

2.4. Molecular dynamics simulation

The molecule was firstly solvated with TIP3P explicit water molecules in a box of 72 × 75 × 58 Å. Eight Na^+ ions were added to ensure electrostatic neutrality. Missing parameters for the ligand were added using the CHARMM22 force field [36]. The NAMD software [37] was used to simulate the dynamic behavior of the complex using the par_all27_prot_lipid_na.inp parameter file from CHARM22 and under periodic boundary conditions. Long-range electrostatics was evaluated using the particle-mesh Ewald approach [38]. Simulations were carried out in the NPT ensemble using Langevin dynamics and piston to fix temperatures (300 K) and pressure (1 atm). Hydrogen-heavy atom bonds were constrained to their equilibrium values with the SHAKE algorithm [39]. The system was first energy minimized (6400 conjugate gradient steps) and then equilibrated (500 ps) before recording the trajectory. MD trajectory frames were recorded at 1 ps intervals, for a simulation total of 5 ns.

Molecular representations, secondary structure, root mean square deviations (RMSD) and radius of gyration (Rgyr) analysis were performed by Visual Molecular Dynamics (VMD; [40]). The graphics (RMSD and Rgyr) were plotted using GraphPad Prism 5 (GraphPad Software Inc.). The Ramachandran statistics was generated with Discovery Studio Visualizer 3.1 (Accelrys Inc.).

2.5. Alignment and functional annotation

The amplified sequences were aligned, together with two antarease-like transcripts from *Centruroides noxius* [41] and a venom metalloprotease (VMP1) from *M. eupeus*. Pfam (http://pfam.sanger.ac.uk/) and ProScan (http://www.proscan.org/) were used to confirm the conservation of a functional protein domain, as well as the zinc binding sites, the active residues and disulfide bridges. The alignment was visualized with Jalview (http://www.jalview.org/).

2.6. Phylogenetic analysis

Poorly aligned amino acid positions were eliminated from the global alignments using GBlocks allowing the parameters recommended for a low stringency selection [42]. The best nucleotide (JTT + G) and amino acid (WAG) models were determined with MEGA5, and the corresponding phylogenies were constructed following the Maximum Likelihood method with 100 bootstrap replicates.

Additionally, a pairwise codon-based test of neutrality was performed. The number of synonymous (dS) and non-synonymous (dN) substitutions per site was calculated and the variance of the difference dN − dS was computed using the bootstrap method (500 replicates). With this information, we tested the null hypothesis of strict neutrality (H0: dN = dS) using a Ztest with MEGA5 [43]. All positions containing gaps and missing data were eliminated, resulting in a total of 204 positions in the final data set.

3. Results and discussion

3.1. Nucleotide sequence analysis

From cDNA libraries several sequences were amplified that correspond to antarease-like Zn-metalloproteases. From the *T. serrulatus* cDNA library two different sequences were amplified: TserMP_A (GenBank KC693035), and TserMP_B (GenBank KC693036). For *T. pachyurus*, TpachMP_A (GenBank KC693037) and TpachMP_B (GenBank KC693038) were obtained. For *Tityus* sp. four different sequences were generated: TspMP_A (GenBank KC693039), TspMP_B (GenBank KC693040), TspMP_C (GenBank KC693041) and TspMP_D (GenBank KC693042). The sequence for *T. trivittatus* was TrivMP_A (GenBank KC693043) and for *T. fasciolatus*, TfasMP_A (GenBank KC693044).

The translation of the cDNA sequences obtained for *T. serrulatus* allows completing the originally reported partially sequenced antarease, since there was a region of 8 amino acids that the authors were unable to determine [27]. This region is completely conserved for the two *T. serrulatus* clones sequenced. Fig. 1 shows the cDNA sequence of antarease TserMP_A and its deduced amino acid sequence, now completed. The protein sequence that we predict by translation corresponds more closely to the one deposited in the UniProt Database (accession number P86392). Still, in both originally reported sequences Glu183 is missing.

The pairwise comparison of the nucleotide and amino acid sequences shows clear differences between species from distant genera (Table 1). Indeed, the VMP1 protein from *M. eupeus* shares between 35 and 45% identity with the rest of the antarease-like transcripts from *Tityus* and *Centruroides*, whereas the identities between sequences from these two scorpion genera range from 65 to 70% and 52 to 72% at the nucleotide and protein levels, respectively. Based on the sequence identity, two ecogeographic *Tityus* groups can already be distinguished: *T. trivittatus*, *T. fasciolatus* and *T. serrulatus* conform the first group, having more than 90% identity at the nucleotide and amino acid levels, and *T. pachyurus* and *Tityus* sp. on the second group, sharing between 70 and 80% identities in both cases. This classification was further confirmed by the phylogenetic analysis (see below). Additionally, the test of neutrality between nucleotide sequences indicates an over-representation of synonymous substitutions per site (Table 2) as the difference dN − dS takes negative values. Interestingly, the neutrality hypothesis was rejected with statistical support (highlighted p-values < 0.05 on Table 2) for the pairwise comparisons of *T. serrulatus*_B and *T. trivittatus*/*T. fasciolatus*, and between *T. pachyurus* and *T.* spp. Thus, we can suggest that purifying selection is acting, removing deleterious alleles from the metalloprotease genes, within (but not necessarily between) ecogeographic *Tityus* groups in South America.

```
  1      GAY  GAY  TGY  ATH  GTN  GTN  GAR  TAY  TAY  ATH  GTA  ACT  GAC  AGC  GCA  TTT  ACG  AAA  CGC  TTC  AAA  TCA  AAT  TCA  GCT  TTG  ACG  AAC  TAC   87
  1        D    D    C    I    V    V    E    Y    Y    I    V    T    D    S    A    F    T    K    R    F    K    S    N    S    A    L    T    N    Y   29
  1   D    D    D    C    I    V    V    E    Y    Y    I    V    T    D    S    A    F    T    K    R    F    K    S    N    S    A    L    T    N    Y   30

 88  GTA  ACC  GTT  ATG  TTC  ACG  GGG  GTT  CAG  AAT  CTG  ATG  GAT  ACG  TTG  GAG  CTG  GGA  ATA  GGA  GTT  CGT  TTG  CTC  GGA  GTT  ACA  ACA  TTT  ACT  177
 30    V    T    V    M    F    T    G    V    Q    N    L    M    D    T    L    E    L    G    I    G    V    R    L    L    G    V    T    T    F    T   59
 31    V    T    V    M    F    T    G    -    -    -    -    -    -    -    -    E    L    G    I    G    V    R    L    L    G    V    T    T    F    T   52

178  GAA  AAA  ACG  GAA  CCG  TCA  TTT  ATC  AAA  GAC  AAT  CTG  ATT  CCG  GGT  CCT  CCC  GCG  GCT  TTC  GAT  CCT  GAT  GTA  TTA  ATT  TCA  GCT  ATG  TCA  267
 60    E    K    T    E    P    S    F    I    K    D    N    L    I    P    G    P    P    A    A    F    D    P    D    V    L    I    S    A    M    S   90
 53    E    K    T    E    P    S    F    I    K    D    N    L    I    P    G    P    P    A    A    F    D    P    D    V    L    I    S    A    M    S   82

268  AAA  TAT  TAC  TGT  AAT  CAC  CAA  ACT  GGA  TTG  GCT  AAG  GAT  ACT  GAT  CTA  ATT  TTT  CTT  ATT  ACT  GCT  CGT  GGC  ATG  GGC  GAC  CCG  AGA  GAA  357
 90    K    Y    Y    C    N    H    Q    T    G    L    A    K    D    T    D    L    I    F    L    I    T    A    R    G    M    G    D    P    R    E   120
 83    K    Y    Y    C    N    H    Q    T    G    L    A    K    D    T    D    L    I    F    L    I    T    A    R    G    M    G    D    P    R    E   112

358  GAC  GGC  ACC  GTT  GAT  ATA  AAT  ACT  GCA  GGC  ATT  GCA  AAT  AGC  GCT  GGT  GTT  TGC  AAG  CCA  TGT  TTT  AAA  TCT  GGA  ATC  GCT  ACG  GAC  GAT  447
120    D    G    T    V    D    I    N    T    A    G    I    A    N    S    A    G    V    C    K    P    C    F    K    S    G    I    A    T    D    D   150
113    D    G    T    V    D    I    N    T    A    G    I    A    N    S    A    G    V    C    K    P    C    F    K    S    G    I    A    T    D    D   142

448  TCG  GAC  TAC  AAC  GAA  AGA  GTT  GAT  ACA  CTA  GCT  CAC  GAA  TCA  GTG  CAT  TTA  CTC  GGA  AGC  CCT  CAC  GAT  GGC  GAA  GGT  CCC  AAT  CTA  GTC  537
150    S    D    Y    N    E    R    V    D    T    L    A    H    E    S    V    H    L    L    G    S    P    H    D    G    E    G    P    N    L    V   180
143    S    D    Y    N    E    R    V    D    T    L    A    H    E    S    V    H    L    L    G    S    P    H    D    G    E    G    P    N    L    V   172

538  AGC  TTG  GAA  GGC  AGT  CCA  GGA  GCA  GCA  AAT  TGC  CCC  GCA  AAA  GCC  GGT  TAT  ATT  ATG  GGA  AAT  CGT  AAC  GAC  AAA  AAC  AAA  TAC  AAA  TTT  627
180    S    L   E    G    S    P    G    A    A    N    C    P    A    K    A    G    Y    I    M    G    N    R    N    D    K    N    K    Y    K    F   210
173    S    L    -    G    S    P    G    A    A    N    C    P    A    K    A    G    Y    I    M    G    N    R    N    D    K    N    K    Y    K    F   201

628  TCC  CCT  TGT  ACA  AAG  AAA  TGC  GTT  GAA  TAT  CTG  TTA  TCG  AAA  CCC  ACA  GCT  TCC  TGY  ATH  TTY  CAR  CAR  TGY  WSN  GAY   705
210    S    P    C    T    K    K    C    V    E    Y    L    L    S    K    P    T    A    S    C    I    F    Q    Q    C   X    D  236
202    S    P    C    T    K    K    C    V    E    Y    L    L    S    K    P    T    A    S    C    I    F    Q    Q    C    S    D  227
```

Fig. 1. The complete *T. serrulatus* antarease sequence as deduced from the cDNA. The first line is the cDNA sequence from TserMP_A. The second line corresponds to the translated cDNA sequence. The third line is the antarease (UniProtKB P86392) sequence reported by Fletcher et al., 2010. The 5′ and 3′ sections of the cDNA are replaced by the sequence of the degenerated primers used for amplification (shown underlined), since there the sequence of the cDNA is dictated by those primers and is meaningless. The first Asp (D, in bold and italics) in the antarease P86392 sequence was excluded from the forward primer's design. Shown in bold and italics are also Glu183, missing in the originally reported sequence, and amino acid 235 (shown as X) which can be any of the amino acids encoded by the highly degenerated WSN codon (Ser, Thr, Arg, Cys or Trp) of the primer.

3.2. Protein structure and functional description

In functional terms, the protein domain search revealed a high conservation of an ADAM metalloprotease domain (Peptidase_MA clan CL0126). This type of transmembrane proteins contains both a disintegrin and a metalloprotease domain; many of them have the zinc protease pattern, which locates the active site of these proteases. As they contain an adhesion domain and a protease domain, ADAM proteins potentially have both cell adhesion and protease activities [44]. They also share the metalloprotease and disintegrin domains with the disintegrin class of peptides that are present in snake venom [45]. Together, they form the adamlysin/reprolysin subfamily of the metzincin superfamily of Zn-dependent metalloproteinases. As depicted in Fig. 2, the sites for zinc binding, the active residue and the cysteines are conserved in all the considered sequences, except for the case of *T. fasciolatus*, in which a cysteine is absent.

The zinc-dependent metalloproteases, among them the metalloproteases secreted by the salivary glands of arthropods, hold a consensus hydrophobic motif (HExxHxxGxxHx) of the reprolysins family that coordinates zinc, and contains the catalytic Glu, and a distally located methionine (usually 25 residues distal to the first H of the zinc-binding domain) [46]. Because of these two conserved characteristics (Met and the longer zinc-binding motif), this MP family is also known as the metzincins [47]. The ten *Tityus* sequences have the zinc-binding domain of metzincins and a methionine, which is 37 residues distally located from the first H of the zinc-binding domain.

The metzincin superfamily can be further classified in 4 families, which are distinguished by the residue following the third histidine in the zinc ligand motif, and the residues nearby the methionine in the Met-turn [47]. Those proteins having an aspartic acid after the histidine, as the *Tityus* species sequences, belong to the reprolysin family that includes several snake venom proteases, including hemorrhagic toxin and non-hemorrhagic proteins. The reprolysin family proteins do not possess the fifth zinc-ligand, consequently the zinc is tetrahedrally coordinated [48]. However, differently than reprolysins, which have a conserved proline in the Met-turn (consensus sequence CIMXP), the *Tityus* sequences have either an asparagine or a threonine in this position. Despite that, the methionine-containing turn presents similar conformation to the snake venom proteases (SVMP) from reprolysin family.

3.3. Structural modeling, molecular dynamics and analysis

To investigate whether the predicted sequence could adopt the specific fold of the reprolysin family, it was decided to build a model for the

Table 1
Percentage identity for metalloproteases.

	Meup	CnoxA	CnoxB	TpachA	TpachB	TsppA	TsppB	TsppC	TsppD	TserA	TserB	Ttriv	Tfas
Meup	*	61	61	59	60	56	55	57	55	58	58	58	58
CnoxA	45	*	98	66	66	65	67	66	66	70	70	70	70
CnoxB	45	97	*	67	66	66	67	66	67	70	70	70	70
TpachA	37	56	57	*	99	87	87	87	87	70	69	69	70
TpachB	36	55	56	99	*	86	87	87	87	71	71	71	70
TsppA	35	53	54	79	77	*	99	99	98	71	71	71	69
TsppB	35	54	54	80	79	98	*	99	99	70	70	71	69
TsppC	36	54	55	80	78	98	99	*	99	71	71	72	69
TsppD	35	53	54	80	78	98	99	99	*	70	69	70	69
TserA	40	62	62	60	59	53	54	55	54	*	98	94	95
TserB	40	62	62	60	59	53	54	55	54	99	*	94	94
Ttriv	39	60	61	58	58	53	53	54	54	92	93	*	96
Tfas	39	59	60	59	58	53	53	54	54	92	92	94	*

Below diagonal: amino acid identities; above diagonal: nucleotide identities.

Table 2
Codon-based test of neutrality for analysis between sequences.

	CnoxA	CnoxB	TserA	TserB	Ttriv	Tfas	TpachA	TpachB	TsppD	TsppA	TsppC
CnoxA	*	−1.151	−4.933	−4.834	−5.139	−5.257	−6.073	−5.982	−5.7	−5.453	−5.839
CnoxB	0.252	*	−4.744	−4.622	−4.967	−5.062	−5.811	−5.723	−5.459	−5.281	−5.596
TserA	0	0	*	−2.762	−1.401	−1.801	−1.803	−1.821	−1.4	−1.486	−1.341
TserB	0	0	0.007	*	−2.226	−2.177	−1.902	−1.918	−1.517	−1.6	−1.461
Ttriv	0	0	0.164	0.028	*	−0.406	−0.647	−0.658	−0.65	−0.625	−0.478
Tfas	0	0	0.074	0.031	0.685	*	−1.299	−1.311	−1.288	−1.385	−1.266
TpachA	0	0	0.074	0.06	0.519	0.196	*	−0.093	−2.596	−2.318	−2.2
TpachB	0	0	0.071	0.057	0.512	0.192	0.926	*	−2.224	−1.949	−1.81
TsppD	0	0	0.164	0.132	0.517	0.2	0.011	0.028	*	−1.997	−1.707
TsppA	0	0	0.14	0.112	0.533	0.169	0.022	0.054	0.048	*	−0.519
TsppC	0	0	0.183	0.147	0.634	0.208	0.03	0.073	0.09	0.604	*

The probability of rejecting the null hypothesis of strict-neutrality (dN = dS) (below diagonal) is shown. Values of P less than 0.05 are considered significant at the 5% level and are highlighted. The statistic test (dN − dS) is shown above the diagonal.

putative TtrivMP_A and further simulates its behavior in aqueous conditions by molecular dynamics simulations.

Phyre2 [33] analysis identified an X-ray structure of a M12B family zinc metalloproteinase-disintegrin kaouthiagin-like from *Naja atra* [49], PDB ID 3K7N, as the best template with 100% confidence. The best scoring model obtained from the Phyre2 server was then subjected to molecular dynamics simulations for refining and stability verification. By measuring the root mean square deviations (RMSD; Fig. 3A, black line and scale), we verified the model stability over the 5 ns of simulation. We can observe that the model attained stability after the first 1.5 ns, after which no significant structural deviations occurred (average RMSD was 2.39 ± 0.51 Å). In a similar fashion, the radius of gyration (Rgyr) provides information about the model compactness, also correlating with stability. As we can see, the radius of gyration (Fig. 3A, red line and scale) slightly raises over the simulation time, indicating relaxation instead of unfolding (average Rgyr was 17.78 ± 0.25 Å). Together with results from the secondary structure analysis (Fig. 3B), where all of the secondary elements were kept during the entire simulation, this indicates that our modeling strategy was successful, enabling us to compare our structure with known homologues deposited in databases. The Ramachandran statistics at the last frame of the simulation also corroborates model credibility, with over 98% residues in allowed region and only 3 residues in disallowed regions (1.3%). During the entire simulation, the zinc ion added to the predicted metal-binding site remained closely coordinated by the three histidines (His163, 167 and 173) from the HEXXHXXGXXH motif, as well as the putative catalytically active glutamic acid (Glu164) and the conserved methionine (Met200) [50] (Fig. 4), supporting that TtrivMP_A may indeed adopt this predicted fold.

The Met-turn provides a hydrophobic environment for the zinc ion and the three ligating histidine residues at the catalytic centers of these enzymes. It also commonly contains a tyrosine residue that is important for catalysis [50], found at position 198 in the mature TtrivMP_A sequence. Thus, we propose that this model may correspond to a catalytically active conformation of TtrivMP_A.

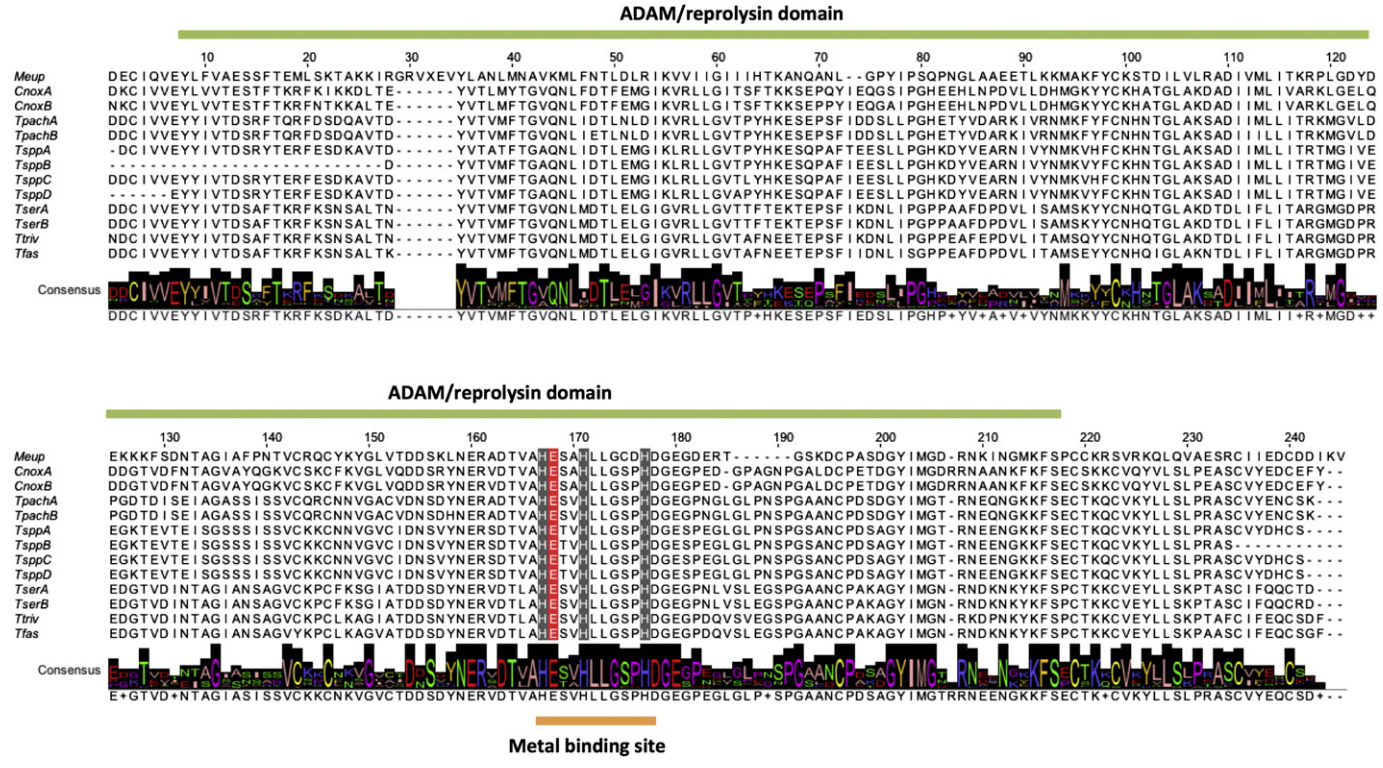

Fig. 2. Amino acid alignment of the metalloprotease domain. The zinc binding sites (gray), and active residue (red) are shown. The ADAM/reprolysin domain and the metal binding site are also delimited.

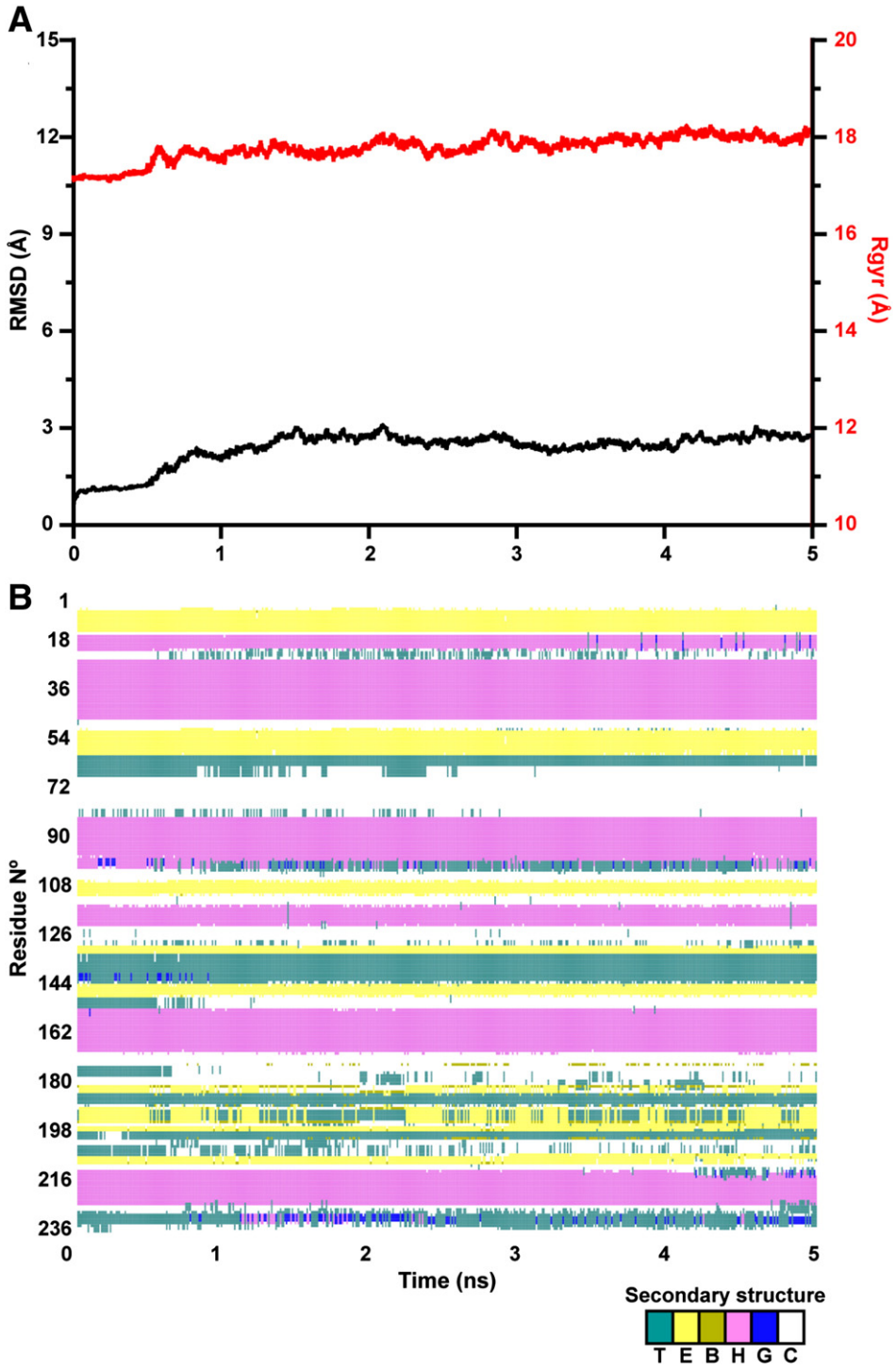

Fig. 3. TtrivMP_A model stability as verified by molecular dynamics simulations. (A) RMSD values (black line) and Rgyr (red line) from the protein backbone during the 5 ns simulation. (B) Secondary structure composition over time, where the β-sheet components turn (T) and extended conformation (E) are represented in teal and yellow, respectively; isolated bridges (B) are in dark yellow; α-helix (H) in pink, 3–10 helix (G) in blue and random coils (C) in white.

3.4. Phylogeography

The species coverage in this study allowed us to examine the metalloprotease transcripts from a phylogenetic perspective, unveiling an interesting correlation between the geographic localization of the species and the conservation of the amino acid residues (Fig. 5).

From the tree topologies, it is easy to observe the evolutionary distance between *Centruroides*, *Tityus* and *Mesobuthus* sequences. All the metalloproteases obtained from the *Tityus* species are clustered in one single group with high bootstrap values, and the distinction between allopatric populations becomes clear as two different clades are formed: one of them containing *T. trivittatus*, *T. fasciolatus* and *T. serrulatus* that are distributed in the south-central region of South America (Argentina and Brazil), and the second one, *T. pachyurus* and *Tityus* sp., distributed in Northern South America and Central America (Colombia, Panama and Costa Rica). The transcripts

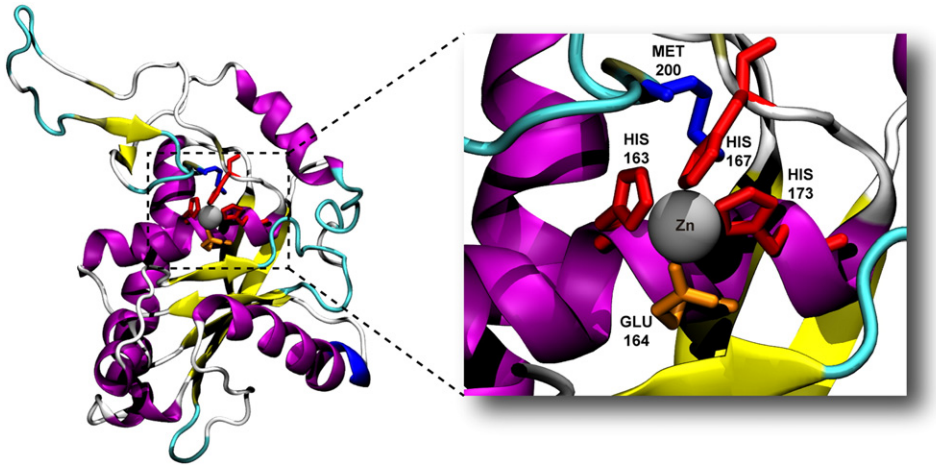

Fig. 4. Structural model of TtrivMP_A obtained after 5 ns of molecular dynamics simulations. The zinc-binding site residues are depicted by red (histidines), orange (glutamic acid) and blue (methionine) sticks. Zinc ion is shown as VDW in gray. Secondary structures were colored accordingly to the same scheme as Fig. 3B. Figure produced with VMD.

from *Centruroides noxius*, which is distributed in North America (Mexico), form an independent clade and, as expected, VMP1 from *M. eupeus*, which is distributed in the Asian continent, behaves as the outgroup in both topologies.

These observations could suggest that the environmental conditions, in which the *Tityus* species live, are playing an important role in the level of conservation of these venom components. Recently, a phylogenetic study of *Tityus* scorpion Na^+-channel modulators revealed a strong separation between the species *T. pachyurus*, *Tityus obscurus*, *T. discrepans* and *T. zulianus* occurring in the Northern part of the Amazon Basin and those living in its Southern part, such as *T. serrulatus*, *T. bahiensis*, *T. stigmurus*, *Tityus costatus* and *T. fasciolatus* [51], reinforcing that ecogeographical differences in the American scorpion habitats have contributed to the speciation process and the diversification of molecular components in scorpion venoms. Moreover, from a population genetics perspective, we can speculate that the geographic separation caused by the Amazon Basin led to an allopatric speciation within the *Tityus* genus followed by other sympatric speciation events at both sides of the Basin. Afterwards, the emergence of two independent zones of geographic overlap for several *Tityus* species could have facilitated successive, random inter-species hybridizations that ultimately, have maintained a high degree of conservation of the venom components within defined regions. This will need to be validated in future studies that should aim to date speciation events and also, to understand the reproductive barriers established in scorpion species.

4. Conclusion

The cDNA sequences coding for putative antarease-like Zn-metalloproteases were amplified from every species that we analyzed. Besides the previously reported sequences for *M. eupeus*, and *C. noxius*, positive results were obtained with five different *Tityus* species. This indicates that these metalloproteases are ubiquitous to a broad range of scorpion species, at least those of the Buthidae family. From our phylogeographic approach, it becomes clear that scorpion venom components reflect the ecogeographic constrains acting on scorpions and lead to important questions about speciation and diversification of the species to be addressed in the future. The molecular model generated from one of the reported sequences suggests that these enzymes could be catalytically active venom components. If the antarease-like subfamily of Zn-metalloproteases proves to be involved in the development of acute pancreatitis, as suggested by Fletcher et al., these proteins would have to be considered as targets for the development of

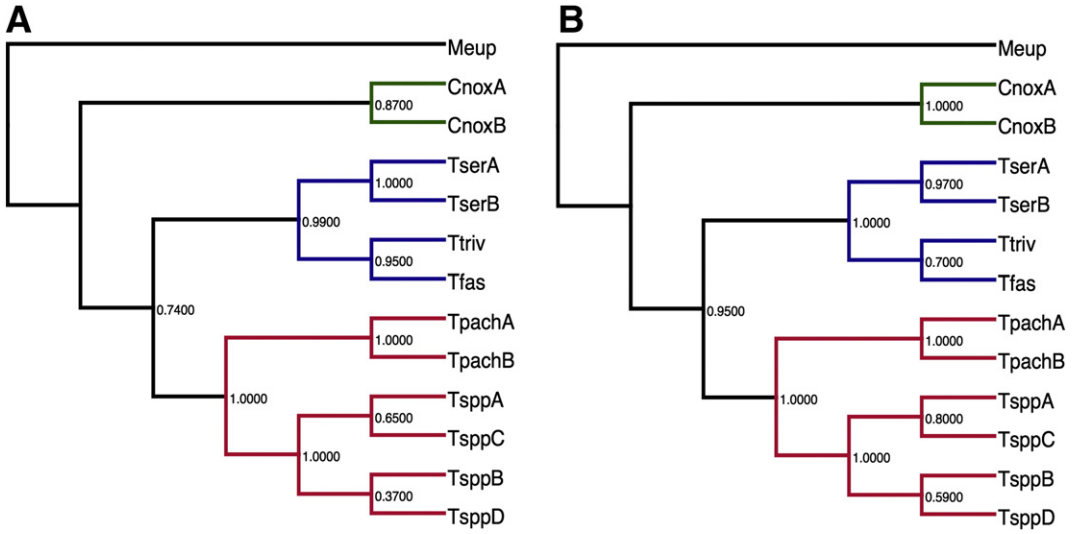

Fig. 5. Tree topologies of the amino acid (A) and nucleotide (B) sequences. Bootstrap values >0.5 are shown. Red: Northern South American and Central American species; blue: South American species; green: North American species.

antivenom therapies that aim at neutralizing the toxic effect of the venom components. If the ideal antivenom is a cocktail of a few highly specific antibodies against the main toxic components of a venom, as compared to the nowadays polyclonal-based therapies [52], then antarease-like Zn metalloproteases should be included in the list of the target antigens.

Funding

This work was partially supported by grants of *Consejo Nacional de Ciencia y Tecnología* (Mexico) (number SEP153496 to LDP) and a bilateral agreement with *Conselho Nacional de Desenvolvimento Científico e Tecnológico* of Brazil (to EFS and LDP), and grant number 306524/2012-0 (to EFS). Additional funding came from *Dirección General de Asuntos del Personal Académico* of the National Autonomous University of Mexico (grant number IN-200113 to LDP).

Acknowledgments

We are in debt with Thalita S. Camargos, Jimmy Guerrero-Vargas, Harry Morales-Duque and Claudia J. Arenas for their contributions to the construction of the *T. fasciolatus*, *T. pachyurus* and *Tityus* sp. cDNA libraries. We thank Adolfo R. de Roodt for providing the *T. trivittatus* specimen and Elia Diego-García for the construction of the *T. trivittatus* cDNA library. We thank Timoteo Olamendi for the DNA sequencing.

References

[1] L.D. Waterman, Some notes on scorpion poisoning in Trinidad, Trans. R. Soc. Trop. Med. Hyg. 31 (1938) 607–624.
[2] C. Bartholomew, Acute scorpion pancreatitis in Trinidad, Br. Med. J. 1 (1970) 666–668.
[3] T. Poon-King, I. Mohammed, R. Cox, E.V. Potter, N.M. Simon, A.C. Siegel, D.P. Earle, Recurrent epidemic nephritis in South Trinidad, N. Engl. J. Med. 277 (1963) 728–733.
[4] R. Otero, E. Navio, F.A. Cespedes, M.J. Nunez, L. Lozano, E.R. Moscoso, C. Matallana, N.B. Arsuza, J. Garcia, D. Fernandez, J.H. Rodas, O.J. Rodriguez, J.E. Zuleta, J.P. Gomez, M. Saldarriaga, J.C. Quintana, V. Nunez, S. Cardenas, J. Barona, R. Valderrama, N. Paz, A. Diaz, O.L. Rodriguez, M.D. Martinez, R. Maturana, L.E. Beltran, M.B. Mesa, J. Paniagua, E. Florez, W.R. Lourenco, Scorpion envenoming in two regions of Colombia: clinical, epidemiological and therapeutic aspects, Trans. R. Soc. Trop. Med. Hyg. 98 (2004) 742–750.
[5] P.L. Fletcher Jr., M.D. Fletcher, L.D. Possani, Characteristics of pancreatic exocrine secretion produced by venom from the Brazilian scorpion, *Tityus serrulatus*, Eur. J. Cell Biol. 58 (1992) 259–270.
[6] J.C. Machado, J.F. da Silveira Filho, Indução de pancreatite hemorrágica aguda no cão por veneno escorpiônico de T. serrulatus, Mem. Inst. Butantan 40–41 (1977) 1–9.
[7] G. Novaes, O.L. Catanzaro, W.T. Beraldo, L. Freire-Maia, Effect of purified scorpion toxin (tityustoxin) on the pancreatic secretion of the rat, Toxicon 20 (1982) 847–853.
[8] L.D. Possani, B.M. Martin, M.D. Fletcher, P.L. Fletcher Jr., Discharge effect on pancreatic exocrine secretion produced by toxins purified from *Tityus serrulatus* scorpion venom, J. Biol. Chem. 266 (1991) 3178–3185.
[9] G. D'Suze, C. Sevcik, M. Ramos, Presence of curarizing polypeptides and a pancreatitis-inducing fraction without muscarinic effects in the venom of the Venezuelan scorpion *Tityus discrepans* (Karsch), Toxicon 33 (1995) 333–345.
[10] A. Borges, E. Trejo, A.M. Vargas, G. Cespedes, A. Hernandez, M.J. Alfonzo, Pancreatic toxicity in mice elicited by *Tityus zulianus* and *Tityus discrepans* scorpion venoms, Invest. Clin. 45 (2004) 269–276.
[11] M. Gueron, R. Yaron, Cardiovascular manifestations of severe scorpion sting. Clinicopathologic correlations, Chest 57 (1970) 156–162.
[12] S. Sofer, H. Shalev, Z. Weizman, E. Shahak, M. Gueron, Acute pancreatitis in children following envenomation by the yellow scorpion *Leiurus quinquestriatus*, Toxicon 29 (1991) 125–128.
[13] K.R. Murthy, J.D. Medh, B.N. Dave, Y.E. Vakil, F.R. Billimoria, Acute pancreatitis and reduction of H + ion concentration in gastric secretions in experimental acute myocarditis produced by Indian red scorpion, *Buthus tamulus*, venom, Indian J. Exp. Biol. 27 (1989) 242–244.
[14] M.D. Fletcher, L.D. Possani, P.L. Fletcher Jr., Morphological studies by light and electron microscopy of pancreatic acinar cells under the effect of *Tityus serrulatus* venom, Cell Tissue Res. 278 (1994) 255–264.
[15] P.L. Fletcher, M. Fletcher, L.K. Fainter, D.M. Terrian, Action of New World scorpion venom and its neurotoxins in secretion, Toxicon 34 (1996) 1399–1411.
[16] M.V. Gomez, C.R. Diniz, Separation of toxic components from the Brazillian scorpion *Tityus serrulatus* venom, Mem. Inst. Butantan 33 (1966) 899–902.
[17] E.C. Arantes, S.V. Sampaio, C.A. Vieira, J.R. Giglio, What is tityustoxin? Toxicon 30 (1992) 786–789.
[18] A.P. Corrado, A. Antonio, C.R. Diniz, Brazilian scorpion venom (*Tityus serrulatus*), an unusual sympathetic postganglionic stimulant, J. Pharmacol. Exp. Ther. 164 (1968) 253–258.
[19] L. Freire-Maia, M.C. Ferreira, Estudo do mecanismo da hiperglicemia e da hipertensão arterial, produzidas pelo veneno de escorpião, no cão, Mem. Inst. Oswaldo Cruz 59 (1961) 11–22.
[20] S.A. Ibrahim, Phospholipase A in scorpion venoms, Toxicon 5 (1967) 59–60.
[21] N.A. Valdez-Cruz, C.V. Batista, L.D. Possani, Phaiodactylipin, a glycosylated heterodimeric phospholipase A from the venom of the scorpion *Anuroctonus phaiodactylus*, Eur. J. Biochem. 271 (2004) 1453–1464.
[22] R.B. Nair, P.A. Kurup, Investigations on the venom of the South Indian scorpion *Heterometrus scaber*, Biochim. Biophys. Acta 381 (1975) 165–174.
[23] L. Borchani, A. Sassi, D. Shahbazzadeh, J.M. Strub, H. Tounsi-Guetteti, M.S. Boubaker, A. Akbari, A. Van Dorsselaer, M. El Ayeb, Heminecrolysin, the first hemolytic dermonecrotic toxin purified from scorpion venom, Toxicon 58 (2011) 130–139.
[24] C.V. Batista, S.A. Roman-Gonzalez, S.P. Salas-Castillo, F.Z. Zamudio, F. Gomez-Lagunas, L.D. Possani, Proteomic analysis of the venom from the scorpion *Tityus stigmurus*: biochemical and physiological comparison with other *Tityus* species, Comp. Biochem. Physiol. C Toxicol. Pharmacol. 146 (2007) 147–157.
[25] F.M. Almeida, A.M. Pimenta, S.G. De Figueiredo, M.M. Santoro, M.F. Martin-Eauclaire, C.R. Diniz, M.E. De Lima, Enzymes with gelatinolytic activity can be found in *Tityus bahiensis* and *Tityus serrulatus* venoms, Toxicon 40 (2002) 1041–1045.
[26] M.F. Martin-Eauclaire, B. Ceard, A.M. Ribeiro, C.R. Diniz, H. Rochat, P.E. Bougis, Biochemical, pharmacological and genomic characterisation of Ts IV, an alpha-toxin from the venom of the South American scorpion *Tityus serrulatus*, FEBS Lett. 342 (1994) 181–184.
[27] P.L. Fletcher Jr., M.D. Fletcher, K. Weninger, T.E. Anderson, B.M. Martin, Vesicle-associated membrane protein (VAMP) cleavage by a new metalloprotease from the Brazilian scorpion *Tityus serrulatus*, J. Biol. Chem. 285 (2010) 7405–7416.
[28] I. Amaro, L. Riano-Umbarila, B. Becerril, L.D. Possani, Isolation and characterization of a human antibody fragment specific for Ts1 toxin from *Tityus serrulatus* scorpion, Immunol. Lett. 139 (2011) 73–79.
[29] L. Riano-Umbarila, G. Contreras-Ferrat, T. Olamendi-Portugal, C. Morelos-Juarez, G. Corzo, L.D. Possani, B. Becerril, Exploiting cross-reactivity to neutralize two different scorpion venoms with one single chain antibody fragment, J. Biol. Chem. 286 (2011) 6143–6151.
[30] E.J. Venancio, F.C. Portaro, A.K. Kuniyoshi, D.C. Carvalho, G. Pidde-Queiroz, D.V. Tambourgi, Enzymatic properties of venoms from Brazilian scorpions of *Tityus* genus and the neutralisation potential of therapeutical antivenoms, Toxicon 69 (2013) 180–190.
[31] E. Diego-Garcia, E.F. Schwartz, G. D'Suze, S.A. Gonzalez, C.V. Batista, B.I. Garcia, R.C. de la Vega, L.D. Possani, Wide phylogenetic distribution of scorpine and long-chain beta-KTx-like peptides in scorpion venoms: identification of "orphan" components, Peptides 28 (2007) 31–37.
[32] S.F. Altschul, W. Gish, W. Miller, E.W. Myers, D.J. Lipman, Basic local alignment search tool, J. Mol. Biol. 215 (1990) 403–410.
[33] L.A. Kelley, M.J. Sternberg, Protein structure prediction on the web: a case study using the Phyre server, Nat. Protoc. 4 (2009) 363–371.
[34] S.F. Altschul, T.L. Madden, A.A. Schaffer, J. Zhang, Z. Zhang, W. Miller, D.J. Lipman, Gapped BLAST and PSI-BLAST: a new generation of protein database search programs, Nucleic Acids Res. 25 (1997) 3389–3402.
[35] J. Soding, Protein homology detection by HMM–HMM comparison, Bioinformatics 21 (2005) 951–960.
[36] B.R. Brooks, C.L. Brooks III, A.D. Mackerell Jr., L. Nilsson, R.J. Petrella, B. Roux, Y. Won, G. Archontis, C. Bartels, S. Boresch, A. Caflisch, L. Caves, Q. Cui, A.R. Dinner, M. Feig, S. Fischer, J. Gao, M. Hodoscek, W. Im, K. Kuczera, T. Lazaridis, J. Ma, V. Ovchinnikov, E. Paci, R.W. Pastor, C.B. Post, J.Z. Pu, M. Schaefer, B. Tidor, R.M. Venable, H.L. Woodcock, X. Wu, W. Yang, D.M. York, M. Karplus, CHARMM: the biomolecular simulation program, J. Comput. Chem. 30 (2009) 1545–1614.
[37] J.C. Phillips, R. Braun, W. Wang, J. Gumbart, E. Tajkhorshid, E. Villa, C. Chipot, R.D. Skeel, L. Kale, K. Schulten, Scalable molecular dynamics with NAMD, J. Comput. Chem. 26 (2005) 1781–1802.
[38] T. Darden, D. York, L. Pedersen, Particle mesh Ewald—an N.log(N) method for Ewald sums in large systems, J. Chem. Phys. 98 (1993) 10089–10092.
[39] J.P. Ryckaert, G. Ciccotti, H.J.C. Berendsen, Numerical-integration of Cartesian equations of motion of a system with constraints—molecular-dynamics of N-alkanes, J. Comput. Phys. 23 (1977) 327–341.
[40] W. Humphrey, A. Dalke, K. Schulten, VMD: visual molecular dynamics, J. Mol. Graph. 14 (33–38) (1996) 27–38.
[41] M. Rendon-Anaya, L. Delaye, L.D. Possani, A. Herrera-Estrella, Global transcriptome analysis of the scorpion *Centruroides noxius*: new toxin families and evolutionary insights from an ancestral scorpion species, PLoS One 7 (2012) e43331.
[42] G. Talavera, J. Castresana, Improvement of phylogenies after removing divergent and ambiguously aligned blocks from protein sequence alignments, Syst. Biol. 56 (2007) 564–577.
[43] K. Tamura, D. Peterson, N. Peterson, G. Stecher, M. Nei, S. Kumar, MEGA5: molecular evolutionary genetics analysis using maximum likelihood, evolutionary distance, and maximum parsimony methods, Mol. Biol. Evol. 28 (2011) 2731–2739.
[44] T.G. Wolfsberg, P. Primakoff, D.G. Myles, J.M. White, ADAM, a novel family of membrane proteins containing A disintegrin and metalloprotease domain: multipotential functions in cell–cell and cell–matrix interactions, J. Cell Biol. 131 (1995) 275–278.
[45] P. Primakoff, D.G. Myles, The ADAM gene family: surface proteins with adhesion and protease activity, Trends Genet. 16 (2000) 83–87.
[46] N.D. Rawlings, A.J. Barrett, Evolutionary families of metallopeptidases, Methods Enzymol. 248 (1995) 183–228.
[47] N.M. Hooper, Families of zinc metalloproteases, FEBS Lett. 354 (1994) 1–6.

[48] W. Bode, F.X. Gomis-Ruth, W. Stockler, Astacins, serralysins, snake venom and matrix metalloproteinases exhibit identical zinc-binding environments (HEXXHXXGXXH and Met-turn) and topologies and should be grouped into a common family, the 'metzincins', FEBS Lett. 331 (1993) 134–140.
[49] H.H. Guan, K.S. Goh, F. Davamani, P.L. Wu, Y.W. Huang, J. Jeyakanthan, W.G. Wu, C.J. Chen, Structures of two elapid snake venom metalloproteases with distinct activities highlight the disulfide patterns in the D domain of ADAMalysin family proteins, J. Struct. Biol. 169 (2010) 294–303.
[50] N.D. Rawlings, A.J. Barrett, A. Bateman, MEROPS: the database of proteolytic enzymes, their substrates and inhibitors, Nucleic Acids Res. 40 (2012) D343–D350.
[51] J.A. Guerrero-Vargas, C.B. Mourao, V. Quintero-Hernandez, L.D. Possani, E.F. Schwartz, Identification and phylogenetic analysis of *Tityus pachyurus* and *Tityus obscurus* novel putative Na+-channel scorpion toxins, PLoS One 7 (2012) e30478.
[52] G.P. Espino-Solis, L. Riano-Umbarila, B. Becerril, L.D. Possani, Antidotes against venomous animals: state of the art and prospectives, J. Proteomics 72 (2009) 183–199.